ELSEVIER

Thermochimica Acta 280/281 (1996) 83–100

thermochimica acta

Diffuse interface model of volume nucleation in glasses[1]

László Gránásy

Research Institute for Solid State Physics, H-1525 Budapest, POB 49, Hungary

Abstract

A diffuse interface theory (DIT) of nucleation is applied for the crystallization of various oxide glasses showing volume nucleation. It is demonstrated that, in contrast with the classical theory which often yields "anomalous" nucleation prefactors, the DIT is consistent with the experiments. A method is outlined for distinguishing homogeneous and volumetric heterogeneous nucleation mechanisms.

Keywords: Diffuse interface; Glass; Model; Nucleation

1. Introduction

Crystallization in a pure liquid or glass starts with homogeneous nucleation [1], i.e. small crystal-like particles (heterophase fluctuations) appear through stochastic processes, of which those smaller than a critical size (20 to a few hundred molecules, depending on the undercooling and the excess free energy from the interface region) dissolve with a high probability, while the larger ones are able to grow leading eventually to bulk crystallization. This picture is supported by computer simulations [2] and calculations from first principles [3]. The formation of heterophase fluctuations is often catalyzed by foreign particles distributed in the volume, or by the presence of surfaces and container walls (bulk- or surface-induced heterogeneous nucleation, respectively).

Since these processes (especially the heterogeneous ones) play an essential role in a number of high technology applications, e.g. low thermal expansion glass ceramics for the aerospace industry, optical memories, artifical teeth and bones, cryopreserva-

[1] Dedicated to Professor Hiroshi Suga.

SSDI 0040-6031(95)02637-1

tion, etc., a quantitative description would be of both scientific and practical importance.

With a few exceptions, the theoretical approaches belong to two main groups: (i) the classical nucleation theory (CNT) and its descendants, and (ii) the field theoretical models. In materials science, nucleation experiments are interpreted almost exclusively in terms of the CNT. However, this approach is not without problems [1]. The nuclei are considered as particles showing bulk properties, assuming thus an extremely sharp interface. In contrast, computer simulations [4] and more advanced theories [3, 5] predict interfaces of several molecular layers thick, implying that the CNT may be seriously in error. Indeed, the comparison with field theoretical calculations reveals substantial deviations at deep undercoolings [3]. Unfortunately, a direct experimental test of the CNT cannot be performed, since one of the input parameters, the interfacial free energy, γ, of the undercooled crystal–liquid interface cannot be measured independently of nucleation. Another difficulty is the almost inevitable presence of volumetric heterogeneities that catalyze nucleation. An indirect test is still possible knowing the nucleation rate I as a function of temperature T, and having a guess at the temperature dependence of γ: the classical expression for the rate of bulk heterogeneous nucleation is $I \approx x_N I_{0,\mathrm{hom}} \exp\{-W^*_{\mathrm{hom}} f(\theta)/kT\}$, where $x_N \leq 1$ is the fraction of molecules active on the surface of heterogeneities, $I_{0,\mathrm{hom}}$ and $W^*_{\mathrm{hom}} = (16\pi/3)\gamma^3(\Delta g_0^+)^{-2}$ are the prefactor and work of formation for a homogeneous process, respectively, Δg_0^+ is the volumetric Gibbs free energy difference between the bulk phases, k is Boltzmann's constant, and $f(\theta)$ accounts for the reduction in W by the heterogeneities, while θ is the contact angle between the crystal–melt and crystal–heterogeneity interfaces. Then, plotting $\lg(I/I_{0,\mathrm{hom}})$ vs. $X_{\mathrm{CNT}} = \chi_\gamma^3(\Delta g_0^+)^{-2}T^{-1}$ ("consistency plot"), where $\chi_\gamma = \gamma(T)/\gamma(T_f)$, one should obtain a straight line intersecting the vertical axis at $\lg x_N$ with a slope proportional to $f(\theta)\gamma(T_f)^3$. For more than the past 40 years, this analysis has been performed for various substances (oxide glasses [1, 6], molten metals [7] and water [8]). It is now well established that the assumption $\chi_\gamma = 1$ leads to unphysical x_N values (10^6–10^{49}) known as "anomalous nucleation prefactors". Obviously, $x_N \leq 1$. This problem has not been resolved unambiguously so far. Although the "anomalous prefactors" can be removed assuming a suitable temperature dependence (increasing linearly with T [1, 6–8]) or curvature dependence [8, 9] of γ (at the expense of introducing further adjustable parameters), in the light of the problems mentioned above it seems probable that an unphysical x_N indicates a general failure of the classical approach. This view is strongly supported by the fact that in the case of vapor condensation, where γ is known with a high accuracy, the predicted and measured nucleation rates deviate by several orders of magnitude [10].

Unfortunately, the more advanced field theoretical models of crystal nucleation [3] require a knowledge of the Helmholtz free energy as a function of a suitably chosen order parameter for all intermediate states between the equilibrium states, a relationship known for only a few specific model systems (mean-field Ising model, van der Waals gas, regular solution, etc.). It is generally inaccessible for experiments, while its calculation from first principles requires numerous approximations, thus bearing a substantial error. Furthermore, the square gradient approximation applied in Ref. [3] is valid for only smooth order parameter changes through the interface,

a condition which may be unrealistic for the crystal–liquid interface, as happened for vapor condensation far from the critical point [11]. In summary, a well-proven quantitative description of nucleation is not yet available; thus a different approach, which accounts for interface diffuseness, may be of some interest.

Such a theory [12], relating W to a characteristic thickness δ of the interface, expressible in terms of bulk properties, has been proposed recently (Diffuse Interface Theory, DIT) for both homogeneous [12a–e] and heterogeneous [12f] nucleation. It has been shown that, near equilibrium, the DIT and CNT are equivalent, while far from equilibrium the DIT gives an improved description of the experiments [12b, d]. For example, without introducing free parameters the DIT describes the condensation of non-polar vapors remarkably better than the CNT [12a, b]. Predicting a size-dependent γ, which results in an apparent temperature dependence of γ for the undercooled crystal–melt interface [12c], the DIT is expected to remove "anomalous" nucleation prefactors. Its ability to do so has been demonstrated on pure metals (Hg, Ga) and on $Li_2O{\cdot}2SiO_2$ glass [12c, d, f]. Further tests on other substances would be essential to clarify the applicability range of the DIT. The most pronounced "anomalies" were reported for oxide glasses. Therefore, in the present work literature data on crystal nucleation in five oxide glasses are analyzed in terms of the DIT. It will be shown that the DIT is consistent with a variety of experimental data on crystal nucleation and that "anomalous" prefactors do not occur. A unique possibility to distinguish between homogeneous nucleation and a bulk heterogeneous process far from site-saturation is outlined. (Site-saturation is defined as the extinction of heterogeneous nucleation sites as they are used up by advancing nucleation. Accordingly, I decreases and the number density of crystallites N_v approaches a constant value. If heterogeneities are in abundance, the homogeneous and bulk heterogeneous processes cannot be distinguished from the N_v vs. time curve, and an electron microscopic study of the central part of the crystallites is needed).

2. Diffuse interface analysis

It is assumed that the local physical state in the interface region can be characterized by cross-interfacial number density (N), specific internal energy (u) and entropy (s) distributions. Then the work of formation of (spherical) heterophase fluctuations can be given as

$$W_{\text{hom}} = \int_0^\infty \{\Delta h^+(r,T) - T\Delta s^+(r,T)\} 4\pi r^2 \mathrm{d}r \tag{1}$$

where $\Delta h^+(r,T) = N(r,T)\{[u(r,T) - u_0] + p_0[v(r,T) - v_0]\}$, $\Delta s^+(r,T) = N(r,T)\{s(r,T) - s_0\}$, p_0 is the external pressure, v is the molecular volume and the subscript 0 denotes the parent phase. Eq. (1) is equivalent to the respective equation of the field theoretical approach [3]; however, instead of using the square gradient approximation and solving the Euler equation for the order parameter profile, we relate W to a characteristic thickness expressible in terms of bulk physical properties. The procedure is illustrated on interfacial distributions calculated for the vapor–liquid inter-

face of water at $T = 273$ K by the van der Waals/Cahn–Hilliard theory [13]. As pointed out by Turnbull [14], in stable equilibrium (planar interface, Fig. 1a) the area enclosed by the Δh^+ and $T\Delta s^+$ functions is equal to the respective interfacial free energy γ_{plan} (a quantity measurable in equilibrium even for the crystal–liquid interface [15]). Let us introduce step-functions (one for Δh^+ and another for $T\Delta s^+$) of the same integral and amplitude as the original distributions, and choose distance of their positions $\delta = Z_S - Z_H$ as the characteristic thickness. Evidently, the area enclosed by the step-functions is also equal to γ_{plan}, i.e. δ is expressible in terms of measurable quantities: $\delta = \gamma_{plan}/\Delta h_{eq}$, where Δh_{eq} is the volumetric heat of transformation. Eq. (1) for spherical fluctuations can also be evaluated in terms of the amplitude ($\Delta h_0^+ = \Delta h^+(r \to 0)$, $\Delta S_0^+ = \Delta s^+(r \to 0)$) and position ($R_H$, R_S) of the step-functions corresponding to distributions in the unstable equilibrium (nucleus, Fig. 1b): $W_{hom} = \kappa\{R_H^3 \Delta h_0^+ - R_S^3 T\Delta s_0^+\}$, where $\kappa = 4\pi/3$. Note that this expression is still equivalent to Eq. (1). A simple diffuse interface model of nucleation can be obtained assuming that (i) bulk properties exist at least in the center of the fluctuations (the amplitudes are related to bulk thermodynamic properties), and (ii) the interface diffuseness is essentially independent of undercooling (as expected from structural models of the crystal–liquid interface [16]), i.e. $R_S - R_H \approx \delta$. Maximizing W_{hom} with respect to size, the work of formation and size of nuclei are $W_{hom}^* = -\kappa\delta^3 \Delta g_0^+ \psi$ and $R_S^* = \delta \cdot \{1 + q\}\eta^{-1}$, where $\psi = 2(1+q)\eta^{-3} - (3+2q)\eta^{-2} + \eta^{-1}$, $q = (1-\eta)^{1/2}$, $\eta = \Delta g_0^+/\Delta h_0^+$ and $\Delta g_0^+ = \Delta h_0^+ - T\Delta s_0^+$. A similar model containing additional free parameters was proposed recently (F. Spaepen, Mater. Sci. Eng., A178 (1994) 15; F. Spaepen, Solid State Phys., 47 (1994) 1).

For the nucleation of congruently melting compounds, Δh_0^+ and Δs_0^+ can be calculated from the heat of fusion ΔH_f, melting point T_f and specific heat difference ΔC_p

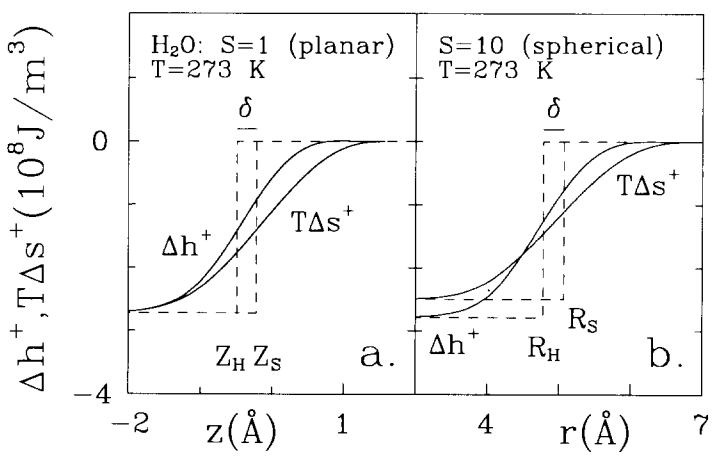

Fig. 1. Interfacial distributions and the definition of the characteristic thickness δ in (a) stable and (b) unstable equilibrium. (The distributions were calculated for the liquid–vapor interface using the Van der Waals/Cahn–Hilliard theory [13]. $S = p_0/p_e$ is the supersaturation, while p_0 and p_e are the external and the equilibrium pressure.)

using the formulae $\Delta h_0^+ = -\{\Delta H_f + \int_{T_f}^{T} \Delta C_p \mathrm{d}T\} v_m^{-1}$ and $\Delta s_0^+ = -\{\Delta H_f/T_f + \int_{T_f}^{T} [\Delta C_p/T] \mathrm{d}T\} v_m^{-1}$, where v_m is the molar volume of the crystal. $\Delta C_p = C_p^g - C_p^c$, where superscripts g and c stand for the glass and the crystal, respectively; note that for crystal nucleation (as for vapor condensation) $\Delta h_0^+, \Delta s_0^+, \Delta g_0^+ < 0$, while $R_S - R_H = \delta > 0$.)

Following the classical route, the nucleation rate for a homogeneous mechanism can be given as $I_{hom} = I_{0,hom} \exp\{-W_{hom}^*/kT\}$, where $I_{0,hom} = NO\Gamma Z$[1], as in case of the CNT, except that the new formulae for the work of formation and the size of nuclei are used ($O = N_s A^*$, N_s is the surface density of molecules, $A^* = 4\pi R^{*2}$ is the surface area of nuclei, $\Gamma = 6D/\lambda^2$, D is the diffusion coefficient calculated here from the viscosity μ using the Stokes–Einstein relation, λ is the jump distance of molecules, while the factor $Z = \{(2\pi kT)^{-1} |\mathrm{d}^2 W_{hom}/\mathrm{d}i^2|_{i^*}\}^{1/2}$ accounts for the dissolution of nuclei, i is the number of molecules in the fluctuation, and superscript * denotes quantities referring to the nucleus). Although, in case of the DIT, the relation between the work of formation of heterogeneous and homogeneous nuclei is more complex than in the CNT [12f], e.g. a formal introduction of $f(\theta)$ in the DIT is acceptable only if the ratio of the volumetric and surface contributions to W_{het}^* is roughly independent of θ, i.e. near $\theta = 1/2\pi$, an analysis of bulk heterogeneous nucleation implies that in analogy to its classical counterpart, the plot of $\lg(I/I_{0,hom})$ vs. $X_{DIT} = -\Delta g_0^+ \psi T^{-1}$ can be used to assess x_N [12f]. Here, the slope is proportional to δ_{eff}^3, where δ_{eff} is an apparent characteristic thickness equal to δ in the case of homogeneous nucleation and smaller otherwise. Since $I_{0,hom}$ weakly depends on δ, a self-consistent plot can be found by a simple iteration scheme: first calculate $\lg(I/I_{0,hom})$, with a rough estimate of δ, determine δ from the slope, then recalculate $\lg(I/I_{0,hom})$, determine δ again, etc. The process converges rapidly. The assessed x_N can be used to test the applicability of nucleation theories. As well as $x_N \leq 1$, $x_N = nN_{het}/N$ should satisfy $x_N \geq nx_c$ (with the equality valid for site-saturation), where n is the average number of active molecules on the surface of a heterogeneity, N_{het} is the number density of heterogeneities, $x_c = N_c/N$, while N_c is the maximum number density of crystallites seen in the experiments. Unfortunately, experimental information on n is non-existent. Considering that the most potent nucleation areas (favored by local geometrical or chemical conditions) probably cover only a fraction of the surface of a heterogeneity, the lower limit of n is determined by the contact area between the heterogeneity and the nucleus, which close to either the ideal or the non-wetting limits may be as low as 5–10 molecules. Thus a reasonable criterion of consistency with experiments is $10x_c < x_N \leq 1$.

3. Results and discussion

In this work, five stoichiometric oxide glasses which show volume nucleation are investigated: $Li_2O{\cdot}2SiO_2$ (LS_2), $BaO{\cdot}2SiO_2$ (BS_2) and $Na_2O{\cdot}2CaO{\cdot}3SiO_2$ (NC_2S_3), where "anomalous" prefactors were reported, and two others $Na_2O{\cdot}2SiO_2$ (NS_2) and $CaO{\cdot}Al_2O_3{\cdot}2SiO_2$ (CAS_2), for which no anomaly was found. For the sake of comparison, as well as the results of the DIT, those from the CNT analysis will also be presented. With the exception of LS_2 these compositions melt congruently, but even

LS_2 is completely liquid 1 K above its incongruent melting point, justifying the use of the fomulae for Δh_0^+ and Δs_0^+.

3.1. LS_2

The nucleation rates were taken from Refs. [17–20]. Note that the composition of the glass is critical [1]. If it is made lithia-rich (≥ 35.5 mol%), some lithium metasilicate crystals appear [21]; if it is made lithia-poor (≤ 32.0 mol%), there is a metastable miscibility gap in the undercooled liquid leading to liquid–liquid phase separation. For glasses at exactly the LS_2 composition, crystallization is expected to occur directly to lithium disilicate, without phase separation or other crystalline phase [1]. A recent work indicates, however, that even within 0.4 mol% of the stoichiometric composition, the first-forming phase is a transient phase closely resembling lithium metasilicate [22]. Further investigations are needed to clarify this point. Following previous works [1, 17, 18, 22], thermal properties of the stable phase are used in this analysis. The relevant data, with other physical properties used in the calculations, are listed in Table 1. Of the conflicting thermal data available in the literature [25, 32], the results of Takahashi and Yoshio [25] were adopted, since they are in excellent agreement with a recent value of the heat of crystallization at room temperature, 53.5 ± 4 kJ mol^{-1} by Sen et al. [33] compare 52.7 kJ mol^{-1} in Ref. [25] and less than 45.1 kJ mol^{-1} from the data of Ref. [32]. The $\Delta C_p(T)$ function was obtained by differentiating a polynomial, least-squarefitted to the enthalpy difference from Ref. [25]. The temperature dependence of the viscosity is described by Vogel–Fulcher expressions, $\mu = A \exp\{B/(T[\mathrm{K}] - C)\}$. It is argued [34] that, in order to ensure coherence with experimental incubation times of nucleation, the parameters of Matusita and Tashiro (MT) [24] should be preferred to those of Zanotto and James (ZJ) [17]. The respective consistency plots for the CNT and DIT are shown in Fig. 2, while the relevant data are summarized in Table 2. As noted in former works [17, 18], the plots are essentially straight lines except at low temperatures, where a pronounced downward curvature can be seen. In accord with previous analyses [1, 17, 18], the x_N values from the linear portion of the plots are 17–20 orders of magnitude (o.m.) too high. In constrast, the DIT results are all reasonable, indicating a homogeneous nucleation mechanism, a conclusion fully consistent with the experimental information, e.g. lack of site-saturation, available on the system.

To clarify the significance of these results, both the statistical error of x_N and the uncertainty originating from the experimental error of the input parameters were determined. Leaving the points of the curved section out of the fit, the statistical error is relatively small, about 0.4–1.5 o.m. (CNT) and 0.2–0.7 o.m. (DIT). The results are more sensitive to the viscosity function. The x_N values obtained using the viscosity coefficients of MT and ZJ differ by 4.8–8.5 o.m. and 1.8–3.4 o.m. for the CNT and the DIT, respectively (see Table 2). It is noteworthy that the low temperature curvature of the plots is much reduced using the ZJ viscosity data. This does not imply, however, that the ZJ parameter set should be preferred. A recent work shows that a substantial curvature is present even if the diffusion coefficient is evaluated from the incubation time of nucleation [35] which is exempt from many possible sources of error, e.g. the

Table 1
Physical properties used in the computations

Composition	M/g	λ/Å	ρ/g cm^{-3}	A/Pa s	B/K	C/K	T_f/K	ΔH_f/kJ mol^{-1}	ΔC_p/J mol^{-1} K^{-1}
LS_2	150.05	4.70	2.45[a]	3.63×10^{-11}[24]	7761[24]	460[24]	1307[25]	61.1[25]	$a + bT$[b]
				6.46×10^{2}[17]	3100.7[17]	594.8[17]			
+ water				4.60×10^{1}[c]	3513.6[c]	557.8[c]			
BS_2	273.50	4.96	3.73[a]	6.76×10^{1}[17]	3918.8[17]	794.6[17]	1693[27]	37.5[27]	9.86[d]
NC_2S_3	354.4	5.95	2.80[a]	1.38×10^{-5}[28]	11266.6[28]	547.3[28]	1562[28]	91.2[28]	51.9[28]
+ water				5.13×10^{-7}[e]	16200[e]	430.3[e]			
CAS_2	278.21	5.51	2.76[a]	1.41×10^{-6}[f]	15542.5[f]	738[f]	1826[30]	135.5[30]	$a + bT + cT^2 + dT^3 + eT^4$[g]
NS_2	182.15	5.11	2.27[a]	2.29×10^{-1}[h]	5330.5[h]	541[h]	1147[25]	44.4[25]	$a + bT + cT^2 + dT^3$[i]

[a] The crystal densities are taken from Ref. [23]. [b] From differentiating a polynomial fitted to the enthalpy difference from Ref. [25]: $a = -7.385$, $b = 1.969 \times 10^{-2}$. [c] From a fit to data on glass L5 of Ref. [26]. [d] Average calculated from T_f, the heat ΔH_x [27] and temperature T_x [27] of crystallization, and the ΔH_f assessed from binary phase diagrams as $(\Delta H_f - \Delta H_x)/(T_f - T_x)$. [e] From a fit to data on glass N2 of Ref. [26]. [f] From a fit to experimental data of Ref. [29]. [g] Polynomial fitted to specific heat data Ref. [30]: $a = 10.37$, $b = -8.143 \times 10^{-2}$, $c = 1.616 \times 10^{-4}$, $d = -1.092 \times 10^{-7}$, $e = 2.380 \times 10^{-11}$. [h] From a fit to experimental data of Ref. [31]. [i] From differentiating a polynomial fitted to enthalpy data of Ref. [25]: $a = -96.57$, $b = 1.8846 \times 10^{-1}$, $c = 8.8916 \times 10^{-5}$, $d = -1.4834 \times 10^{-7}$.

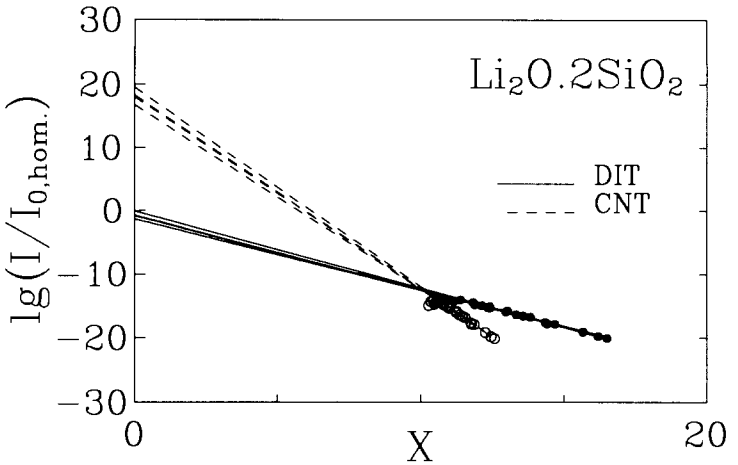

Fig. 2. Determination of x_N from consistency plots of the DIT (solid line) and the CNT (dashed line) for LS_2. ($X_{CNT} = (\Delta g_0^+)^{-2} T^{-1}$ is given in units of $(\Delta H_f/v_m)^{-2} T_f^{-1}$, while $X_{DIT} = -\Delta g_0 \psi T^{-1}$ is presented in units of $\Delta H_f/T_f v_m$. Notations: ○, experimental points with X_{CNT} on the abscissa; ●, the same points with X_{DIT} on the abscissa. Nucleation rate data are from Refs. [17–20].)

Table 2
Lg(x_N) values and interfacial parameters assessed from the "consistency" plots for CNT and DIT

Composition	Sample	$\lg(x_N)^{CNT}$	$\lg(x_N)^{DIT}$	δ_{eff}/Å	α
LS_2	F^{MT}	16.8 ± 0.8	−1.3 ± 0.4	2.23 ± 0.02	0.478
	T^{MT}	18.3 ± 0.8	−0.7 ± 0.4	2.27 ± 0.02	0.486
	ZJ^{MT}	18.0 ± 0.4	−0.8 ± 0.2	2.26 ± 0.01	0.485
	J^{MT}	19.5 ± 0.4	−0.1 ± 0.2	2.29 ± 0.01	0.491
	F^{ZJ}	25.2 ± 1.5	2.0 ± 0.7	2.42 ± 0.03	0.519
	T^{ZJ}	23.3 ± 1.3	1.2 ± 0.6	2.39 ± 0.03	0.511
	ZJ^{ZJ}	25.9 ± 0.9	2.3 ± 0.4	2.44 ± 0.02	0.522
	J^{ZJ}	24.3 ± 0.8	1.7 ± 0.4	2.40 ± 0.02	0.515
BS_2	ZJ	20.1 ± 0.9	−2.0 ± 0.3	2.95 ± 0.03	0.596
	JR	23.8 ± 1.0	−0.7 ± 0.4	3.06 ± 0.03	0.617
NC_2S_3	$C1^{GJ}$	47.2 ± 3.3	−6.7 ± 0.3	3.00 ± 0.03	>0.505
	$G16^{GJ}$	57.1 ± 2.8	−6.4 ± 0.5	3.06 ± 0.06	>0.514
	$N2^{N2}$	63.5 ± 5.6	−6.0 ± 0.5	3.16 ± 0.06	>0.532
	$C1^{N2}$	40.0 ± 2.1	−8.0 ± 0.2	2.89 ± 0.02	>0.484
CAS_2	H	−15.1 ± 0.6	−17.3 ± 0.4	1.14 ± 0.03	>0.207
	C	−16.4 ± 0.4	−19.9 ± 0.3	1.29 ± 0.01	>0.234
NS_2	K	−8.4 ± 0.6	−14.5 ± 0.4	1.31 ± 0.02	>0.256

Notations: F, Ref. [20]; T, Ref. [19]; ZJ, Ref. [17]; JR, Ref. [18]; C1, Ref. [28]; G16, Ref. [38]; N2, Ref. [26]; H, Ref. [42]; C, Ref. [29]; K, Ref. [31]. Superscripts in column 2 indicate the set of viscosity parameters used: ZJ, Ref. [17]; MT, Ref. [24]; GJ, Ref. [28]; N2, fitted to data on high water content N2 glass (see Table 1). The errors shown are standard deviations. For uncertainties of other origin see discussion in text.

application of the Stokes–Einstein relation for highly viscous media, the assumption that bulk and cross-interfacial diffusion is comparable, etc.

The differences in viscosity may originate from minor deviations in the water content, composition, relaxation, etc. Therefore, a further parameter set was evaluated from least-square fitting to viscosity data on a glass containing water in excess. The respective x_N values are about 1 o.m. lower than those calculated with the MT parameters. However, no coherence was found with the incubation times, implying that water content alone cannot account for the differences between the MT and ZJ viscosity data. To investigate the sensitivity for thermal data, ΔH_f and ΔC_p were varied by 10% (a reasonable estimate of the experimental error, though better data are also available for some systems). The resulting changes are of about the same amplitude, (0.5 o.m. for CNT and 0.1 o.m. for DIT), but of opposite sign. The combined uncertainties from all sources amount to 6.3–10.3 o.m. (CNT) and 2.2–4.0 o.m. (DIT), showing that (i) x_N from the CNT is considerably more sensitive to the error of the input data than the value from the DIT, and (ii) even the combined uncertainty cannot explain the presence of "anomalous prefactors". The importance of accurate input data is, however, evident.

3.2. BS_2

Nucleation rates from Refs. [17] and [36] are considered. The first nucleating phase is the high-temperature monoclinic BS_2 (h-BS_2) [37], metastable below 1623 K with respect to the orthorhombic low-temperature phase (l-BS_2). Unfortunately, the thermal data are incomplete. Although ΔH_f (h-BS_2) has been assessed [27] from binary phase diagrams, to the author's knowledge, neither the heat of the h-$BS_2 \rightarrow$ l-BS_2 transformation, nor $\Delta C_p(T)$ has been measured so far. In contrast, the heat ΔH_x and temperature T_x of crystallization is known for l-BS_2 [27]. Thus, an average $\Delta C_p = (\Delta H_f - \Delta H_x)/(T_f - T_x)$ was computed from T_f, ΔH_f, T_x and ΔH_x. Both the CNT and DIT results (and errors) are rather similar to those for LS_2 (see Fig. 3 and Table 1), indicating "anomalous prefactors" (CNT) and a homogeneous nucleation mechanism (DIT). The latter conclusion accords with the lack of site-saturation in the experiments. To see how the error from estimating the specific heat difference may influence the results, the analysis was repeated with Turnbull's approximation $\Delta C_p = 0$ representing the lowest physically meaningful value. In accord with previous work [1], the CNT plot yields lower but still "anomalous" prefactors (about 12.8–15.8 o.m. too high). The DIT plot moves in the opposite direction: the respective $\lg x_N$ values are also positive but much smaller, 1.3–3.0 o.m., still indicating a homogeneous process within experimental error. Doubling ΔC_p, in contrast, increases $\lg x_N^{CNT}$ further (37.6–42.9), while $\lg x_N^{DIT}$ is lowered into the domain of heterogeneous nucleation (-4.7– -5.6).

3.3. NC_2S_3

In addition to the nucleation rates of Refs. [22, 28, 38], the average rates N_v/t_n determined from data of Ref. [26] were also investigated, where N_v is the number

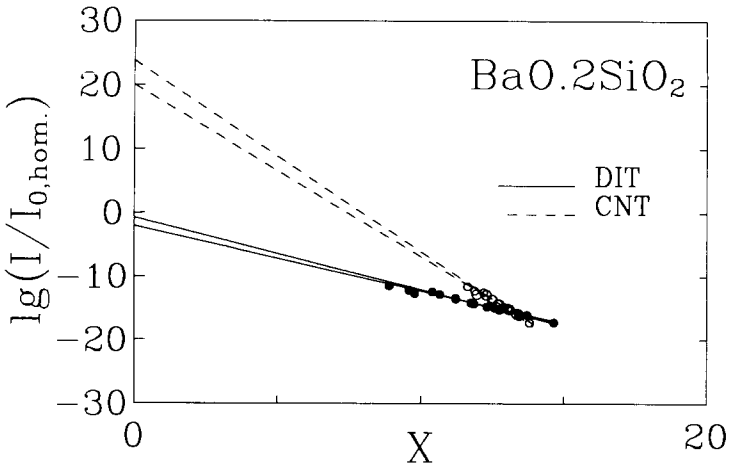

Fig. 3. "Consistency plots" for BS_2 from the CNT and the DIT using nucleation rate data from Refs. [17, 36]. (Units and notations as in Fig. 2.)

density of crystals after a heat treatment period t_n. At high temperatures, the incubation time τ of nucleation is negligible on the time scale of the experiments; therefore $N_v/t_n \approx I$. However, with decreasing temperature τ becomes comparable with t_n leading to an increasing underestimation of I by N_v/t_n [28]. The first nucleating phase is the high-temperature NC_2S_3 modification (*stable* in the temperature range of nucleation experiments) [28,38]. The experimental T_f, ΔH_f and ΔC_p were taken from Ref. [28]. The viscosity coefficients for the pure glass are given in Ref. [28]. A second set was evaluated for increased water content (Table 1). In accord with previous analyses [6, 28], the CNT plots yield enormously high x_N values (about 47–64 o.m. too high, see Fig. 4a and Table 1). A small downward curvature at low temperatures, not unlike the one seen on LS_2, can also be observed. In contrast with previous expectations of a homogeneous nucleation mechanism [28, 38], the x_N values ($\approx 10^{-6.4}$) from the DIT analysis indicate a bulk heterogeneous nucleation (Fig. 4b). The combined uncertainties of $\approx$ 28.4 o.m. for the CNT and $\approx$ 3.2 o.m. for the DIT do not influence the conclusions.

Possible clues of the predicted heterogeneous mechanism were sought among experimental data. A heterogeneous process close to site-saturation can be identified from a leveling of the $N_v(t)$ curve at long times. Similar behavior was observed by Zanotto and Galhardi at 627°C [39]. However, at this temperature crystal growth is important, and $N_v(t)$ can be explained solely by the ingestion of nuclei by growing crystals [39]. Site-saturation is expected to show up at high nucleation rates. Indeed, such a behavior can be seen at the temperature (595°C) of maximum nucleation rate, where the growth rate is too small for perceptible ingestion of nuclei (see insert in Fig. 4b), although the magnitude of the effect is close to the statistical error of the experiments. The respective number density of heterogeneities is about $N_{het} \approx 2.2 \times 10^{15}\,m^{-3}$ ($x_{het} = N_{het}/N = 4.62 \times 10^{-13}$ and $\lg x_{het} = -12.33$), putting

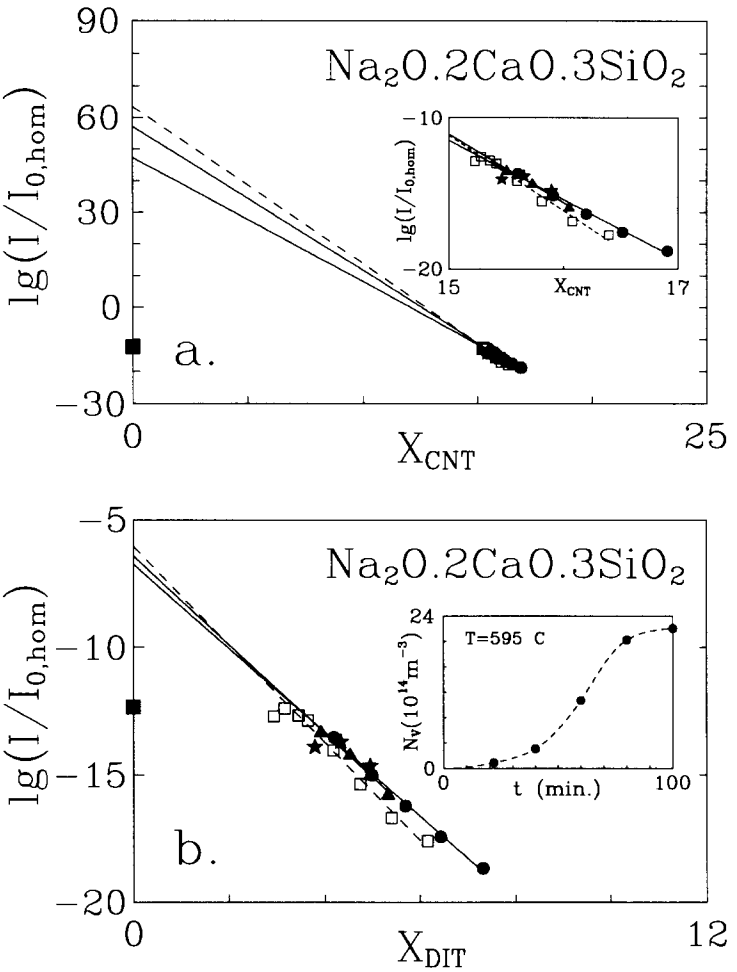

Fig. 4. Assessement of x_N from the CNT (a) and the DIT (b) for NC_2S_3, and results from Ref. [28] implying site-saturation at 595°C (insert in (b)). Notations for (a),(b): solid lines, linear function fitted to points from nucleation rate data (full symbol): ●, C1 glass in Ref. [28]; Δ, G16 glass in Ref. [38]; ★, from Ref. [22]; ■, x_{het} for $N_{het} = 2.2 \times 10^{15}\,m^{-3}$; □, N_v/t_n for glass N2 containing extra amounts of water [26]; dashed line in (a),(b), linear function fitted to the points for N_v/t_n; in insert of (b), line to guide the eyes. Units on the abscissas are as in Fig. 2.

the average diameter of heterogeneities into the (rather wide) range of 0.008–12 μm. The TEM results [40] do not exclude the presence of such particles in the center of crystallites, provided that they are at the lower end of the allowed sizes. A comparison with the assessed $x_N = 10^{-6.4\pm3.2}$ shows that the criterion $10x_{het} < x_N \leq 1$ is satisfied with an ample safety margin. It is worth mentioning that the presence of such nucleation centers could explain a puzzling result obtained by comparing nucleation

kinetics in pure NC_2S_3 and a glass containing ≈ 1 μm Pt precipitates [41]: for short times, the nucleation rate of the Pt containing sample is the higher, but soon after the transient period the pure sample takes over. Were a homogeneous nucleation present in the pure sample, and a homogeneous plus a Pt particle induced process in the other, the nucleation rate in the Pt-containing sample would always be higher. In Ref. [41], small composition differences are held responsible for the unexpected "crossover". Another possibility is that such heterogeneities dominate nucleation in the "pure" glass, which can also catalyze the Pt precipitation. Then, during preparation of the Pt-containing sample, the original heterogeneities are engulfed by Pt particles, completely "erasing" the previous nucleation mode. Accordingly only nucleation on Pt surfaces could be seen later which may have an incubation time and rate different from those of the original process. Although lacking decisive evidence, the experimental information on NC_2S_3 is not inconsistent with the conclusion of the DIT analysis.

3.4. CAS_2

This composition normally crystallizes with surface nucleation. Efforts devoted to finding volume nucleation usually fail [6]. There are only two data sets in the literature on the rate of volume nucleation, one from a direct measurement [42], and another with I evaluated from X-ray detection of crystallinity while assuming constant nucleation and growth rates [29]. The latter method is expected to underestimate I in the presence of transient effects or site-saturation. Indeed, data from the indirect method are lower than those from the direct measurements by about 4.5 o.m., giving a hint of the error involved. (The possibility that substances of different heterogeneity concentrations were used in the two experiments is considered less probable, since the samples were prepared in the same laboratory.) A metastable phase nucleates [42]. However, thermal data are available [30] for only the stable phase (anorthite). The Vogel–Fulcher parameters were determined from a least-square fit to viscosity data of Ref. [29]. The $\lg(I/I_{0,\mathrm{hom}})$ vs. X plots for the CNT and DIT are presented in Fig. 5 and the relevant data are given in Table 2. The x_N values assessed from both the CNT and the DIT analyses (i) indicate a bulk heterogeneous process, and (ii) satisfy the criterion $10x_c < x_N < 1$, where x_c was estimated from the maximum nucleation rate and time ($\lg x_c = -21.6$). The presence of heterogeneous nucleation is supported by the small slope of the plot, yielding δ_{eff} values which are about half of those for other substances of similar molecular size. Also, the closeness of the CNT and DIT plots is expected for heterogeneous processes close to ideal wetting [12f]. In summary, the range of data suggest a heterogeneous mechanism as did the DIT (and the CNT) analysis. Note, that the present results for the CNT deviate considerably from those in Refs. [29] and [42], which indicate a homogeneous nucleation mechanism. The source of the discrepancy is that instead of Hoffman's expression for the Gibbs free energy difference (known as a rather crude approximation [1]), the measured thermal properties were used here, which demonstrates again the importance of accurate input data.

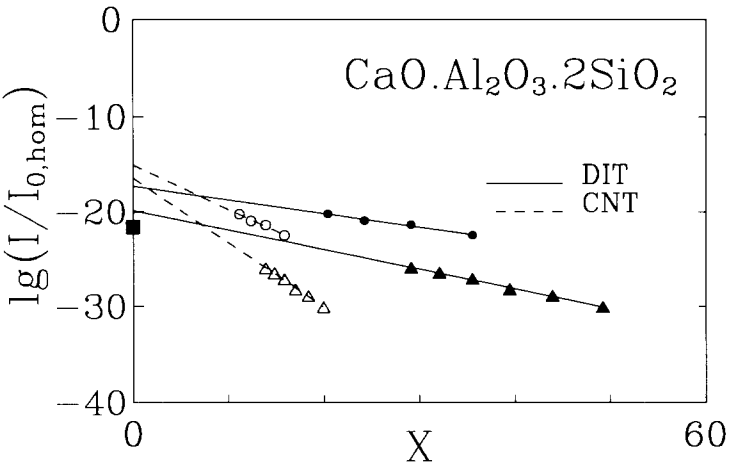

Fig. 5. Estimation of x_N from the DIT and the CNT for CAS_2. Notations: ●, ○, data from direct determination of nucleation rate [42]; ▲, Δ, data from an indirect method [29]; dashed lines and open symbols, CNT; solid lines and full symbols, DIT; ■, x_c estimated from the maximum nucleation rate and time given in Ref. [29]. Units are as in Fig. 2.

3.5. NS_2

Matusita and Tashiro [43] and Scott and Pask [44] observed only surface nucleation for this composition. In the only work on volume nucleation [31], I was determined by the indirect method applied for CAS_2 in Ref. [29], which may underestimate the nucleation rate considerably. Thermal and viscosity data from Refs. [25] and [31] were used to obtain the $\Delta C_p(T)$ and Vogel–Fulcher parameters. As in case of CAS_2, both the CNT and DIT plots indicate a heterogeneous nucleation mechanism (Fig. 6). Here the DIT fit does not meet the condition $10x_c < x_N$, where $\lg x_c = -12.1$ was assessed from the maximum nucleation rate and time given in Ref. [31]. However, the discrepancy (≈ 3 o.m.) is of about the same magnitude as the uncertainty of x_N (see LS_2 and NC_2S_3), rendering the discrepancy insignificant. Another factor acting in the same direction is that the indirect method is expected to underestimate the nucleation rate. Adopting the magnitude indicated for CAS_2 (≈ 4.5 o.m.) may restore $10x_c < x_N$. Thus the results on NS_2 are still compatible with the quantitativity of the DIT. As for CAS_2, other features of the consistency plot (low δ_{eff}, comparable x_N values from the CNT and DIT plots) support the heterogeneous mechanism indicated by the x_N value. Note, that for the same reason as in the case of CAS_2 (experimental thermal data instead of Hoffmann's approximation), the present CNT results differ from those reported in Ref. [31].

Summarizing the investigations of five oxide glasses, it may be concluded that, in contrast with the classical approach which leads to highly unphysical results in the cases of LS_2, BS_2 and NC_2S_3, the DIT is consistent with the experiments examined here. Accordingly, x_N values assessed from the "consistency plot" could be utilized to determine the mechanism of volume nucleation, provided that accurate input data are

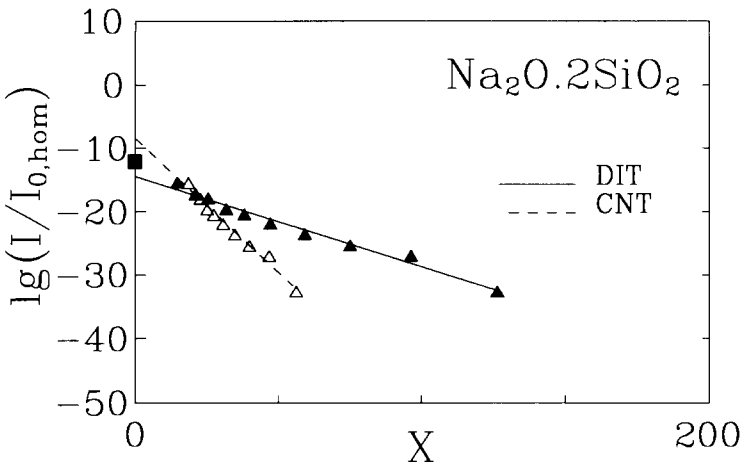

Fig. 6. Determination of x_N from the DIT and the CNT using data from an indirect determination of nucleation rate in NS_2 [31]. Units and notations as in Fig. 5.

available. Experiments under controlled conditions (known x_N) are called for to clarify more accurately the magnitude of errors involved in such a procedure.

A few remarks:

(i) For BS_2 and CAS_2 (and perhaps LS_2), the validity of this analysis rests on the accuracy of approximating the thermal data of the nucleating phase with those of the stable one. Hishinuma and Uhlmann suggested [42] that the differences in the respective data alone may fully account for te appearance of "anomalous prefactors". Considering the extreme sensitivity of the CNT plot for such data [1], this is certainly a possibility that cannot be lightly dismissed. Fortunately, as shown above, the DIT results are much less sensitive to the variation of the input data. Still an experimental determination of the relevant properties of metastable phases would be essential for a more quantitative evaluation of nucleation theories.

(ii) Deviations of the present numerical results from those in Refs. [12c–e] originate from the use of input data of different origin. However, the differences are comparable with the uncertainties given above and do not influence the conclusions.

(iii) The downward curvature at low temperatures seems to be a general feature of the $\lg(I/I_{0,\mathrm{hom}})$ vs. X plot for both the CNT and DIT. A possible explanation is that, with decreasing temperature, the size of the nuclei becomes too small to show bulk properties in their interior, i.e. even the DIT falls out of its validity range. According to the present analysis, the downward curvature starts at nucleus sizes (i^*) which depend on the substance, e.g. LS_2, $i^* < 25$; BS_2, $i^* < 47$; and NC_2S_3, $i^* < 15$.

(iv) Now that the consistence of the DIT with the experiments has been demonstrated, interfacial information can also be extracted from the experiments with some confidence. Since the dimensionless characteristic thickness, $\alpha = \delta/v^{1/3}$, is just the coefficient Turnbull defined through $\gamma = \alpha \Delta H_f N_A^{-1/3} v_m^{-2/3}$, where N_A is the

Avogadro number, it is expected to depend on the crystal structure [16b, 16c, 45, 46]. Note, that only data on homogeneous nucleation can be used, since otherwise an apparent α_{eff} less then the real one would be obtained. The values from the DIT fit are given in the last column of Table 2. They seem to be reasonable, as those for LS_2 and BS_2 are enveloped by the data from direct measurements of γ on Pb (fcc, $\alpha = 0.94$) and H_2O (wurtzite, $\alpha = 0.30$) [15,47] and are comparable with theoretical results for various structures (fcc, $\alpha = 0.86$ [16c], 0.87[5a]; bcc, $\alpha = 0.71$ [45]). Further experiments on homogeneous nucleation are needed to establish a correlation between α and structure, a knowledge of which is essential for quantitative prediction of crystal nucleation in melts and glasses.

(v) Previous work has shown that the problem of "anomalous prefactors" can be removed by assuming either a size-dependent [8,9] or a temperature-dependent [1,6–8] interfacial free energy in the CNT. The necessity of a size-dependent correction to γ for small particles with a diffuse interface was recognized by Gibbs [48]. The first-order correction is often given as $\gamma(r) = \gamma_\infty \{1 - 2\delta_T/R + \ldots\}$ [49], where R is the radius of the particle and δ_T is the Tolman length, a quantity rather difficult to determine, e.g. δ_T for the liquid–vapor interface of a Lennard-Jones molecules could only recently be evaluated with an error of about 50% [50], while δ_T for crystal nucleation is as yet unknown. Thus, these corrected theories contain an extra adjustable parameter, δ_T. Other studies on crystal nucleation [1,6,8] demonstrated that a linear temperature dependence $\gamma(T) = a + b\,T (a, b, > 0)$ may also eliminate the "anomalous" prefactors. Unfortunately, there is not a general way to predict a and b; thus this approach also contains an extra adjustable parameter relative to the DIT.

It can be shown that the DIT is mathematically analogous to a classical theory in which a size-dependent interfacial free energy [12a–c] is used. The combination of this size dependence with the reduction in the size of nuclei with decreasing temperature, yields $\gamma = -\delta \Delta g_0^+ (\psi/4)^{1/3}$ [12b], i.e. γ decreases with increasing undercooling [12c]. The main virtue of the DIT is that, in contrast with other improved models which contain a minimum of two adjustable parameters, it predicts $\gamma(T)$ using a single parameter. Furthermore, this parameter can be fixed provided that the interfacial free energy is measured independently of nucleation at the melting point. Although such measurements are possible, data are available for only a few systems. Typical values evaluated from independent measurements for water and Pb [15, 47] are $\delta = 0.95$ Å and 2.96 Å, respectively.

(vi) Transient and non-isothermal nucleation studies [34, 51–54] could provide further tests for the diffuse interface theory, especially the type of analysis described in Refs. [34] and [51].

4. Summary

Nucleation rates for five oxide glasses displaying volume nucleation were analyzed in terms of the classical and the diffuse interface theory. In accordance with previous works, the CNT analysis on LS_2, BS_2 and NC_2S_3 led to highly unphysical results ($x_N = 10^{17}$–10^{64}) known as "anomalous" nucleation prefactors. In constrast, as dem-

onstrated earlier for undercooled hydrocarbons, metals, and a metallic glass [12], the diffuse interface theory is fully consistent with the experiments, showing no trace of "anomalous" prefactors. Based on the new approach, a unique possibility of distinguishing homogeneous and volumetric heterogeneous processes has been outlined and discussed. The diffuse interface analysis indicates a homogeneous nucleation process for compositions LS_2 and BS_2, and a bulk heterogeneous mechanism for NC_2S_3, CAS_2 and NS_2. In the light of other experimental information, relevant to nucleation in these systems, the conclusions are physically plausible.

Acknowledgements

Professor P.F. James, Prof. E.D. Zanotto and Professor Y. Shiraishi are acknowledged for calling the author's attention to publications containing an essential part of the experimental information used in this work. This research was started during the tenure of an Alexander von Humboldt Research Fellowship the author spent in the Institut für Raumsimulation, DLR, Cologne, Germany. The author wishes to express his thanks to Professor B. Feuerbacher and Dr. D.M. Herlach for their support and kind hospitality, and to Dr. L. Ratke, Professor I. Egry and Dr. D.M. Herlach for the valuable discussions. This work was supported by the Hungarian Academy of Sciences under contracts OTKA-T-017485, OTKA-2933 and OTKA-T-4469.

References

[1] KF. Kelton, Solid State Phys., 45 (1991) 75.
[2] W.C. Swope and H.C. Andersen, Phys. Rev., B41 (1990) 7042.
J.S. van Duijneveld and D. Frenkel, J. Chem. Phys., 96 (1992) 4655.
[3] P. Harrowell and D.W. Oxtoby, J. Chem. Phys., 80 (1984) 1639.
C.K. Bagdassarian and D.W. Oxtoby, J. Chem. Phys., 100 (1994) 2139.
[4] See e.g., B.B. Laird and A.D.J. Haymet, J. Chem. Phys., 91 (1989) 3638; Chem. Rev., 92 (1992) 1819.
[5] See, e.g., (a) W.E. McMullen and D.W. Oxtoby, J. Chem. Phys., 88 (1988) 1967.
(b) W.A. Curtin, Phys. Rev. B, 39 (1989) 6775.
(c) D.W. Marr and A.P. Gast, J. Chem. Phys., 99 (1993) 2024.
(d) R. Ohnesorge et al., Phys. Rev. E, 50 (1994) 4801.
[6] P.F. James, J. Non-Cryst. Solids, 73 (1985) 517.
[7] D. Turnbull, J. Chem. Phys., 20 (1952) 411.
Y. Miyazawa and G.M. Pound, J. Cryst. Growth, 23 (1974) 45.
[8] G.R. Wood and A.G. Walton, J. Appl. Phys., 41 (1970) 3027.
[9] M.C. Weinberg et al., Phys. Chem. Glass., 33 (1992) 99.
[10] See, e.g., P.E. Wagner and R. Strey, J. Chem. Phys., 80 (1983) 5266.
R. Strey et al., J. Chem. Phys., 84 (1986) 2325.
C.H. Hung et al., J. Chem. Phys., 90 (1989) 1856; 92 (1990) 7722.
D. Wright and M.S. El-Shall, 98 (1993) 3369.
[11] F.F. Abraham, J. Chem. Phys., 63 (1975) 157.
[12] (a) L. Gránásy, Europhys. Lett., 24 (1993) 121.
(b) L. Gránásy et al., Scripta Metall. Mater., 30 (1994) 621.

(c) L. Gránásy, J. Non-Cryst. Solids, 162 (1993) 301.
(d) L. Gránásy, Mater. Sci. Eng., A178 (1994) 121.
(e) L. Gránásy, Scripta Metall. Mater., in press.
(f) L. Gránásy et al., Scripta Metall. Mater., 31 (1994) 601.
[13] J.D. Van der Waals, Verhand. Kon. Akad. v. Wetensch. (Ie Sectie) 1 (1983) 1.
J.W. Cahn and J.E. Hilliard, J. Chem. Phys., 28 (1958) 258; 31 (1959) 688.
[14] D. Turnbull, in J.A. Prins (Ed.), Physics of Non-Crystalline Solids, North-Holland, Amsterdam, 1964, p. 41.
[15] See e.g., G.E. Nash and M.E. Glicksmann, Philos. Mag., 24 (1971) 577.
[16] (a) R.H. Ewing, J. Cryst. Growth, 11 (1971) 221.
(b) F. Spaepen, Acta Metall., 23 (1975) 729.
(c) F. Spaepen and R.B. Meyer, Scripta Metall., 10 (1976) 257.
(d) Y. Waseda and W.A. Miller, Trans. Jpn. Inst. Metals, 19 (1979) 546.
[17] E.D. Zanotto and P.F. James, J. Non-Cryst. Solids, 74 (1985) 373.
[18] P.F. James, Phys. Chem. Glass., 15 (1974) 95.
[19] J.J. Tuzzeo, Ph.D. Thesis, Ohio State Univ., USA, 1976.
[20] V.M. Fokin et al., Fiz. Khim. Stekla, 3 (1977) 129.
[21] M.F. Barker et al., Phys. Chem. Glass., 29 (1988) 240.
[22] J. Deubener et al., J. Non-Cryst. Solids, 163 (1993) 1.
[23] E.D. Zanotto and E. Müller, J. Non-Cryst. Solids, 130 (1991) 220.
[24] K. Matusita and M. Tashiro, J. Ceram. Soc. Jpn., 81 (1973) 500.
[25] K. Takahashi and T. Yoshio, J. Ceram. Soc. Jpn. 81 (1973) 534.
[26] J.C.R. Gonzalez-Oliver et al., J. Mater. Sci., 14 (1979) 1159.
[27] E.G. Rowlands and P.F. James, in P.H. Gaskell (Ed.), The Structure of Non-Crystalline Solids, Taylor and Francis, London, 1977, p. 215.
[28] J.C.R. Gonzalez-Oliver and P.F. James, J. Non-Cryst. Solids, 38–39 (1980) 699.
[29] D. Crammer et al., J. Non-Cryst. Solids, 45 (1981) 127.
[30] J.F. Stebbins et al., Contrib. Mineral. Petrol., 86 (1984) 131.
[31] L.C. Klein et al., J. Cryst. Growth, 42 (1977) 47.
[32] JANAF Thermochemical Tables, 2nd edn., 1971, U.S. Dept. of Commerce, Nat. Bur. Standards, Washington D.C.
[33] S. Sen et al., J. Non-Cryst. Solids, 168 (1994) 64.
[34] K.F. Kelton and A.L. Greer, J. Am. Ceram. Soc., 74 (1991) 1015.
[35] M.C. Weinberg and E.D. Zanotto, J. Non-Cryst. Solids, 108 (1989) 99.
[36] P.F. James and E.G. Rowlands, in Phase Transformations, Vol. 2, Part III, Inst. of Metallurgists, Northway House, London, 1979 p. 27.
E.G. Rowlands, Ph.D. Thesis, University of Sheffield, UK, 1976.
[37] M.H. Lewis and G. Smith, J. Mater. Sci., 11 (1976) 2015.
A.H. Ramsden and F.P. James, J. Mater. Sci., 19 (1984) 1406.
[38] C.J.R. Gonzalez-Oliver, Ph.D. Thesis, University of Sheffield, UK, 1979.
[39] E.D. Zanotto and and A. Galhardi, J. Non-Cryst. Solids, 104 (1988) 73.
[40] C.J.R. Gonzalez-Oliver and P.F. James, J. Microsc., 119 (1980) 73.
[41] C.J.R. Gonzalez-Oliver and P.F. James, in J.H. Simmons, D.R. Uhlmann and S.W. Freiman (Eds.), Advances in Ceramics, Am. Ceram. Soc., Columbus, Ohio, 1982, p. 49.
[42] A. Hishinuma and D.R. Uhlmann, J. Non-Cryst. Solids, 95–96 (1987) 449.
[43] K. Matusita and M. Tashiro, J. Non-Cryst. Solids, 11 (1973) 471.
[44] W.D. Scott and J.A. Pask, J. Am. Ceram. Soc., 44 (1961) 181.
[45] C.V. Thompson and F. Spaepen, Acta Metall., 31 (1983) 2021.
C.V. Thompson, Ph.D. Thesis, Harvard University, USA, 1982.
[46] L. Gránásy and M. Tegze, Mater. Sci. Forum, 77 (1991) 243.
L. Gránásy et al., Mater. Sci. Eng., A133 (1991) 577.
[47] S.C. Hardy, Philos. Mag., 35 (1977) 471.
[48] J.W. Gibbs, in The Collected Works of J. Willard Gibbs, Vol. I, Thermodynamics, Longmans and Green, London, 1932, p. 232.

[49] R.C. Tolman, J. Chem. Phys., 17 (1949) 333.
F.P. Buff, J. Chem. Phys., 19 (1951) 1591; 23, (1955) 419.
D.H. Rasmussen, J. Cryst. Growth, 56 (1982) 45.
M.A. Larson and J. Garside, J. Cryst. Growth, 76 (1986) 88.
[50] M.J. Haye and C. Bruin, J. Chem. Phys., 100 (1994) 556.
[51] K.F. Kelton and A.L. Greer, Phys. Rev., B38 (1988) 10089.
[52] K.F. Kelton, J. Non-Cryst. Solids, 163 (1993) 283.
[53] J. Šesták, in Z. Chvoj, J. Šesták and A. Tříska (Eds.), Kinetic Phase Diagrams, Studies in Modern Thermodynamics, Vol. 10, Elsevier, Amsterdam, 1991, Chap. 6.
Z. Kožíšek and Z. Chvoj, ibid., Chap. 7.
[54] T. Kemény and J. Šesták, Thermochim. Acta, 110 (1987) 113.